

# FLOW INDUCED VIBRATIONS OF THE CLIC X-BAND ACCELERATING STRUCTURES

T. Charles, K. Ryan, Dept. of Mechanical Engineering Monash University, Clayton 3800, VIC, Australia  
 M. Boland, Australian Synchrotron, Clayton 3800, VIC, Australia  
 G. Riddone, CERN, Geneva, Switzerland  
 A. Samoshkin, JINR, Dubna, Moscow Region

## Abstract

Turbulent cooling water in the Compact Linear Collider (CLIC) accelerating structures will inevitably induce some vibrations. The maximum acceptable amplitude of vibrations is small, as vibrations in the accelerating structure could lead to beam jitter and alignment difficulties. A Finite Element Analysis model is needed to identify the conditions under which turbulent instabilities and significant vibrations are induced. Due to the orders of magnitude difference between the fluid motion and the structure's motion, small vibrations of the structure will not contribute to the turbulence of the cooling fluid. Therefore the resonant conditions of the cooling channels presented in this paper, directly identify the natural frequencies of the accelerating structures to be avoided under normal operating conditions. In this paper a 2D model of the cooling channel is presented finding spots of turbulence being formed from a shear layer instability. This effect is observed through direct visualisation and wavelet analysis.

## INTRODUCTION

Vibrations in accelerating structures could lead to beam jitter and alignment difficulties and is therefore deserving of attention. Tolerances on vibration are strictest for the quadrupole magnets [1], however the cooling channels of the quadrupoles can be mechanically isolated from the magnet yokes, a design feature which is not possible in the accelerating structures. Therefore a flow induced vibrations study is needed for the Main Beam accelerating structures. An initial study into flow induced vibrations [2] acknowledges that the problem should not be fatal but that it does require experimental study and careful design.

## MODEL SET UP

A 2D model of the TD-26 accelerating structure [3] 6 mm diameter cooling channel was constructed. In order to determine accurately the frequency spectrum, a full 3D model will be required, however the 2D model presented here was used to verify the ANSYS FLUENT [4] model setup (figure 1).

### Governing Equations

The flow field was calculated by solving the Reynolds-averaged Navier-Stokes (RANS) equations,

**07 Accelerator Technology**

**T06 Room Temperature RF**

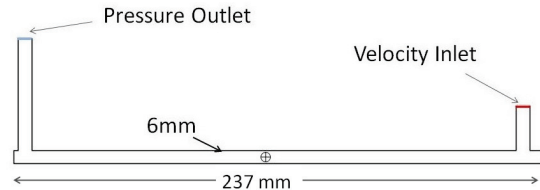


Figure 1: 2D model geometry

$$\frac{\partial u_i}{\partial t} + u_j \frac{\partial u_i}{\partial x_j} = -\frac{1}{\rho} \frac{\partial p}{\partial x_i} + \frac{\partial}{\partial x_j} \left( \frac{\mu}{\rho} \frac{\partial u_i}{\partial x_j} \right) \quad (1)$$

where  $u$  is the velocity and  $\rho$  is the density of the fluid,  $x$  is the position and  $t$  is the time parameter.

The small scale flow structures were not calculated directly but are modeled using the  $k - \omega$  turbulence model, where  $k$  is the turbulent kinetic energy and  $\omega$  represents the specific dissipation rate. The turbulent Reynolds stress tensors were calculated using the Boussinesq approximation in combination with two transport equations [5],

$$\frac{\partial}{\partial t}(\rho k) + \frac{\partial}{\partial x_i}(\rho k u_i) = \frac{\partial}{\partial x_j} \left( \Gamma_k \frac{\partial k}{\partial x_j} \right) + G_k - Y_k \quad (2)$$

$$\frac{\partial}{\partial t}(\rho \omega) + \frac{\partial}{\partial x_i}(\rho \omega u_i) = \frac{\partial}{\partial x_j} \left( \Gamma_\omega \frac{\partial \omega}{\partial x_j} \right) + G_\omega - Y_\omega \quad (3)$$

where  $\rho$  is the density and  $u$  is the velocity of the fluid,  $G_k$  represents the generation of turbulent kinetic energy resulting from the mean velocity gradients,  $G_\omega$  represents the generation of the specific dissipation rate,  $\Gamma_k$  and  $\Gamma_\omega$  represent the effective diffusivity of  $k$  and  $\omega$  respectively and  $Y_k$  and  $Y_\omega$  are the dissipation of  $k$  and  $\omega$  due to turbulence respectively.

### Boundary Conditions

Turbulence onset is dependent upon the value of Reynolds number,

$$Re = \frac{\rho u d}{\mu} \quad (4)$$

where  $\rho$  is the density of the fluid,  $u$  is the velocity,  $d$  is the pipe diameter and  $\mu$  is the dynamic viscosity of the fluid.

For a given pipe diameter transporting water, the Reynolds number is a function only of the fluid velocity. Turbulence onset occurs when the Reynolds number surpasses the critical Reynolds number  $Re_c$ , which is dependent upon the wall roughness of the pipe and flow properties upstream of the pipe [6]. A velocity inlet boundary condition was specified to alter the Reynolds number of the fluid, and the pressure at the outlet was defined.

Boundary conditions for the turbulent variables utilised by the standard  $k-\omega$  model were specified through the hydraulic diameter and the turbulent intensity, which is a ratio of the root-mean-square of the turbulent velocity fluctuations and the Reynolds averaged mean velocity. The turbulent intensity was set to 10% to ensure the fluid lies in the high turbulence regime which is generally specified as 5%-25% [7].

### Spatial and Temporal Discretisation

The time evolution was computed by means of a first order time marching procedure with implicit discretisation. The spatial discretization employed was a second order Upwind scheme for momentum, turbulent energy and specific dissipation rate. In order to resolve the turbulent motion, a relatively small adaptive time step of initially 1e-5 s was employed.

### Grid Resolution Study

A quasi-periodic repetition of the general solution was used as an indication that the simulation had converged and the base line velocity from this was used for a grid resolution study. The quasi periodic condition was reached for all of the mesh sizes shown in table 1. The relative error due to the finite mesh size can be obtained using the solutions within domain of asymptotic convergence with Richardson Extrapolation,

$$P_1 = P^* + \alpha * (\Delta x_1)^\mu \quad (5)$$

where  $P^*$  is the exact solution,  $P_1$  is the solution obtained using a grid spacing of  $\Delta x_1$ ,  $\mu$  is the order of the convergence and  $\alpha$  is an unknown constant.

The order of convergence,  $\mu$  was calculated to be 0.40 which is dependent upon the leading term of the truncation error, therefore the order of the truncation error is 0.40. The global discretisation error is a consequence of the truncation error and, as can be seen from table 1, this error can be reduced by using a finer mesh with a corresponding increased computational cost. Using table 1 it can be calculated that a discretisation error of 5% requires a mesh with approximately 50000 elements.

## RESULTS

The results presented in this section were at the upper limit of Reynolds numbers studied with inlet velocity of 8 m/s. These results were typical of all Reynolds number flows studied. The instability pattern shown in figure

Table 1: Grid resolution study showing the base line velocity converge to the Richardson's extrapolation value of 8.72 m/s.

Velocity Magnitude (m/s) $\pm$ 0.01 m/s	Number of Elements, $\epsilon$	$\frac{1}{\epsilon}$
9.34	20482	$4.88 \times 10^{-5}$
9.26	29472	$3.39 \times 10^{-5}$
9.20	38747	$2.58 \times 10^{-5}$
8.78	50000	$2.00 \times 10^{-5}$
8.72*	-	-

\*Richardson's extrapolation value

2 appears to be a shear layer instability which gives rise to a convective instability. The progression of the shear layer is shown in figure 2. Flow re-circulation arises from the sharp right angle turn in the cooling channel. This creates a shear velocity to become present due to the disparate velocities present. This type of instability is often found at the interface between two fluids of differing velocities. In this case the flow re-circulation was enough to cause the shear layer to form and become unstable.

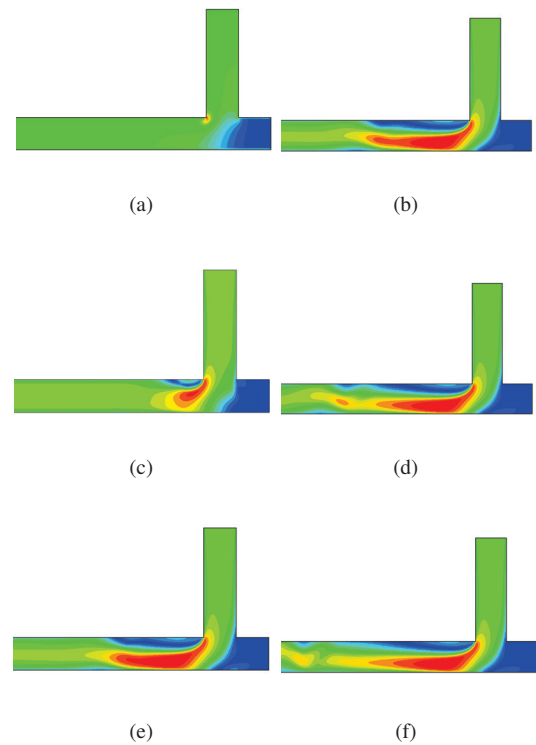


Figure 2: Progression of instability formation at times a)  $4.7 \times 10^{-5}$ s b)  $5.3 \times 10^{-3}$ s c)  $2.3 \times 10^{-3}$ s d)  $6.7 \times 10^{-3}$ s e)  $4.7 \times 10^{-3}$ s f)  $7.8 \times 10^{-3}$ s, where the colour bar varies linearly reaching a maximum of 15.1 m/s

As evident in figure 3, the instability in the shear layer is initiated with a driving frequency which can be found from

performing a Fast Fourier Transform on the signal shown in figure 3b, to be  $1100 \text{ Hz} \pm 50 \text{ Hz}$ .

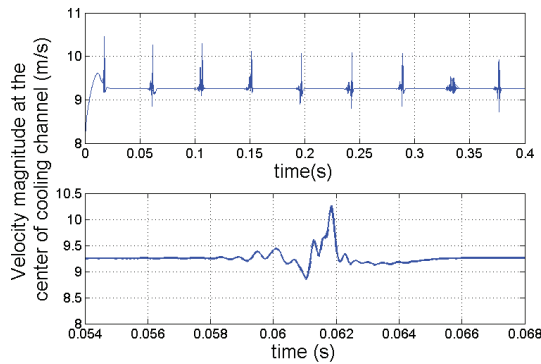


Figure 3: Quasi periodic velocity at the center of the channel, 105 mm from the inlet channel.

### Wavelet Analysis

Figure 4 shows the *DerGauss* wavelet applied to the velocity magnitude in figure 3a [8]. Figure 4 shows clearly the convective nature of the instability. The shear layer which becomes unstable as depicted in figure 2, moves further down the channel, whilst the conditions that helped to form the instability are no longer present. Therefore the low frequency component shown in figure 3 correspond to the time taken for the conditions that produced the instability to be re-established.

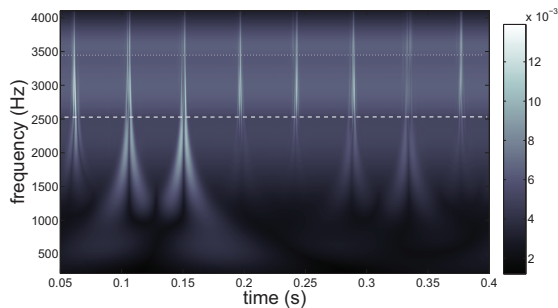


Figure 4: Wavelet Analysis of the quasi periodic velocity data shown in figure 3.

The instability grows to effectively become pockets of white noise, where a spectrum of frequencies is experienced. This is evident in the vertical lines of figure 4. Contributions of approximately 2500 Hz and 3500 Hz are present throughout the entire domain, indicating they are frequencies to be avoided under normal operating conditions at the CLIC Test Facility (CTF3).

### CTF3

The Wavelet and FFT analysis of the cooling channels, indicate that a large range of high frequencies are present,

**07 Accelerator Technology**

**T06 Room Temperature RF**

particularly at the high range of frequencies. The instability formation grows as a result of a low frequency driving force. Therefore, assuming a 3D model will yield similar predictions, in order to avoid natural resonance amplification of this signal the accelerating structure should be mounted under high tension, thus increasing the natural frequency of the structure beyond the low frequency fluid components.

### CONCLUSION

A 2D model of the CLIC TD-26 accelerating structure 6 mm diameter cooling channel was constructed to study the effects of flow induced vibrations. A convective instability arising from a shear layer instability was found to form at the leading edge of the cooling channel. Due to the orders of magnitude difference between the fluid motion and the structure’s motion, vibrations of the structure are assumed not contribute to the turbulence of the cooling fluid. A wide range of frequencies were found to be present as soon as the shear layer became unstable. This effect was always witnessed after a driving frequency  $1100 \text{ Hz} \pm 50 \text{ Hz}$  was experienced, before the turbulent packet convect downstream and are replaced by a relatively unperturbed shear layer. This effect is observed through direct visualisation and wavelet analysis.

### ACKNOWLEDGEMENTS

We acknowledge the support of the IPAC11 organising committee for the EPS-IGA student grant, as well as the Australian Collaboration for Accelerator Science (ACAS) for further financial support.

### REFERENCES

- [1] R. Assmann. “Status of the CLIC Studies on Water Induced Quadrupole Vibrations” CLIC Note 578, CERN-AB-2003-071, 2003.
- [2] W. Schnell “Cooling and Vibrations in the CLIC Main Accelerating Structure” Technical report, CERN-CLIC-NOTE-468, 2001.
- [3] A. Grudiev and W. Wuensch “Design of the CLIC Main Linac Accelerating Structure for CLIC Conceptual Design Report”, LINAC2010, Tsukuba, 2010.
- [4] ANSYS FLUENT Version 13.0 <http://www.ansys.org>.
- [5] D. C Wilcox “Turbulence Modeling for CFD” DCW Industries, Inc., La Canada, California, 1998.
- [6] F. J. Moody “Introduction to Unsteady Thermofluid Mechanics”, New York, Wiley, 1990.
- [7] G. Cole “An introduction to the statistical theory of classical simple dense fluids”, Oxford, Pergamon Press, .
- [8] R. R. Coifman, et al. “Wavelet Analysis and Signal Processing.” In M.B. Ruskai et al., Wavelets and Their Applications, Boston, Jones and Bartlett, 1992.